

## Detection of lung disease using relative reconstruction method in electrical impedance tomography system

Lina Choridah<sup>1</sup>, Riries Rulaningtyas<sup>4</sup>, Lailatul Muqmiroh<sup>3</sup>, Suprayitno<sup>2</sup>, Khusnul Ain<sup>4</sup>

<sup>1</sup>Department of Radiology, Dr. Sardjito Hospital, Faculty of Medicine, Public Health, and Nursing, Universitas Gadjah Mada, Yogyakarta, Indonesia

<sup>2</sup>Department of Physics, Faculty of Science and Technology, Airlangga University, Surabaya, Indonesia

<sup>3</sup>Radiologic Imaging Technology, Faculty of Vocational Studies, Airlangga University, Surabaya, Indonesia

<sup>4</sup>Biomedical Engineering, Faculty of Science and Technology, Airlangga University, Surabaya, Indonesia

### Article Info

#### Article history:

Received Oct 5, 2022

Revised Oct 25, 2022

Accepted Nov 28, 2022

#### Keywords:

Electrical impedance

tomography

Function image

Lung disease

Relative reconstruction method

### ABSTRACT

Lung disease can be diagnosed with the image-based medical devices, including radiography, computed tomography, and magnetic resonance imaging. The devices are very expensive and have negative effects. An alternative device is electrical impedance tomography (EIT). The advantages of EIT are low cost, fast, real-time, and free radiation, so it is very appropriate to be used as a monitoring device. The relative reconstruction method has succeeded in producing functional images of lung anomalies by simulation. In this study, the relative reconstruction method was used to obtain functional images of four lung conditions, namely a healthy person, patient with left lung tumor with organized left pleural effusion, one with pulmonary tuberculosis with right pneumothorax and one with pulmonary tuberculosis with left pleural effusion. The relative reconstruction method can be used to obtain functional images of an individual's lung conditions by using expiratory-respiratory potential data with results that can distinguish between the lungs of a healthy person and a diseased patient, but the position of the lung disease may have less details. The potential data from comparison between the data of a patient and a healthy person can be used as a reference to obtain more accurate functional image information of lung disease.

*This is an open access article under the [CC BY-SA](https://creativecommons.org/licenses/by-sa/4.0/) license.*



### Corresponding Author:

Khusnul Ain

Biomedical Engineering, Faculty of Science and Technology, Airlangga University

Surabaya 60115, Indonesia

Email: [k\\_ain@fst.unair.ac.id](mailto:k_ain@fst.unair.ac.id)

## 1. INTRODUCTION

Lung disease is a condition that prevents the lungs from functioning normally. Some of the most common lung diseases are pneumonia, pulmonary tuberculosis, bronchitis, asthma, chronic obstructive pulmonary disease (COPD), and lung cancer. Recently, the pathogenesis of corona virus disease 2019 (COVID-19) is also associated with disease progression in the lungs [1]. Lung disease can be diagnosed by image-based medical devices, including radiography, computerized tomography (CT)-scan and magnetic resonance imagery (MRI). The devices are very expensive and have side effects if not used carefully, because they use x-ray radiation sources and strong magnetic fields. An alternative electrically based imaging modality is electrical impedance tomography (EIT) [2]. The EIT devices have been widely applied to detect various conditions and diseases [3], [4]. Major heterogeneities in regional ventilation in diseases such as acute respiratory distress syndrome (ARDS), COPD, lung cancer or cystic fibrosis [5], and early detection of pneumothorax can be traced by EIT [6]–[8].

The EIT is a device that can obtain an image of an object's electrical parameters by injecting current and measuring the potential on the object's surface [9], [10]. The electrical potential data are then reconstructed using a certain method to produce an EIT image. The EIT system has several advantages over radiography, CT-scan and MRI. The advantages of EIT are that it is economical, fast, in real-time, radiation-free and non-invasive, so it is very appropriate to be used as a monitoring device [11], [12]. However, one of the disadvantages of EIT is the low resolution of the image [13]. The EIT device is very suitable for use for the purpose of obtaining a functional image [5] or screening. The screening devices are needed by hospitals in areas located far from the main hospital so that they can reduce costs and the risk of delays in handling more serious diseases.

The reconstruction methods can be grouped into two types, namely relative and absolute [14]. The relative methods are one step linearization [15] and back projection, while the absolute method is an iterative method [16]. The relative method has advantages compared to the iterative, namely it is fast and robust. Meanwhile, the weakness is obtaining reference data, but this can be overcome by taking data at a different frequency or time, which is known by the term, data of different frequency or time difference [17]. Therefore, in general, the relative method is used to compare one condition with another, so this method is very appropriate if used to obtain a functional image [16]. EIT is a functional imaging technique that measures the transfer of impedances between electrodes on the body surface to estimate the spatial distribution of electrical properties of tissues. EIT offers many advantages over other neuroimaging technologies, which has led to its potential clinical use [18].

From previous studies, the simulation of relative reconstruction methods has succeeded in producing functional images of the presence of lung anomalies, namely by reconstructing the potential difference between the anomalous lung potential data and the reference lungs, both during inspiration and expiration [19]. In this study, a relative method was proposed to detect the presence of lung disease in the chest cavity. The experiments were conducted on the phantom and the human chest cavity. The method used was to reconstruct the EIT image from anomalous phantom data against normal phantoms and patients with lung disease indications against a healthy person as a reference.

## 2. METHOD

### 2.1. Relative image reconstruction methods

The linearization method assumes that the boundary potential change is a linear function of the conductivity change [20]. The linear function is obtained by approximating the Taylor series on  $V(\gamma)$  around  $\gamma_0$  [21], namely (1):

$$V(\gamma) = V(\gamma_0) + V'(\gamma_0)(\gamma - \gamma_0) + O(\|\gamma - \gamma_0\|^2) \quad (1)$$

where  $V'(\gamma_0)$  is the Jacobion of  $V(\gamma)$  on  $\gamma_0$ . By ignoring the last term, (1) becomes (2):

$$\delta V \approx J \delta \gamma \quad (2)$$

where  $\delta V = V(\gamma) - V(\gamma_0)$ ,  $J = V'(\gamma_0)$  and  $\delta \gamma = \gamma - \gamma_0$ . Jacobion is also known as the sensitivity matrix, so (2) can be written as in (3):

$$[\delta V]_{(q^2 x 1)} = [S]_{(q^2 x p)} [\delta \sigma]_{(p x 1)} \quad (3)$$

where  $[\delta V]$  is the change of boundary potential,  $[S]$  is the sensitivity matrix, and  $[\delta \sigma]$  is the change of conductivity. By manipulating the algebraic formula, (3) can be solved.

However, the  $[S]$  matrix is not square, therefore  $[\delta \sigma]$  cannot be obtained directly, but it is necessary to make a square matrix by multiplying it by the transpose matrix.

$$[S]_{(p x q^2)}^T [\delta V]_{(q^2 x 1)} = [S]_{(p x q^2)}^T [S]_{(q^2 x p)} [\delta \sigma]_{(p x 1)} \quad (4)$$

$$[\delta \sigma]_{(p x 1)} = ([S]^T [S])_{(p x p)}^{-1} [S]_{(p x q^2)}^T [\delta V]_{(q^2 x 1)} \quad (5)$$

Generally  $[S]^T [S]$  is a singular matrix therefore the matrix has no inverse. The problem can be solved by using the Tikhonov formula for regularization [22].

$$[\delta \sigma]_{(p x 1)} = ([S]^T [S] + \lambda I)_{(p x p)}^{-1} [S]_{(p x q^2)}^T [\delta V]_{(q^2 x 1)} \quad (6)$$

where  $\lambda$  is the parameter of regularisation and  $I$  is the identity matrix. The relative imaging methods requires comparison of the potential data as a reference. The reference can be obtained from the reference object's potential data or the object's conductivity changes due to time  $t$  or the object changes due to the frequency  $\omega$ .

The potential data as the reference object is very difficult to obtain, but potential data when the object's conductivity changes with time or because of frequency is very possible to obtain. Referencing the potential data when the object's conductivity changes due to time is called time difference imaging, while referencing the potential data when the object's conductivity changes due to frequency is called frequency difference imaging. The time difference imaging will produce functional images that can be used for physiological monitoring purposes. Time difference imaging has demonstrated its potential as a functional image in several fields of medical applications. The image is only a relative image, and is not an absolute image of the values of  $\sigma$ ,  $\omega$  and  $\omega \in t, \omega$ . This method is more real for the application than absolute imaging.

If time difference data are not obtained, for example, in the progression of breast cancer [23]–[25], then frequency differential imaging can be performed. Admittance spectra of various biological tissues show changes with frequency [26], [27] so that frequency difference imaging is promising to produce an image of the change in admittance distribution. In the different-frequency imaging, the image is constructed from a relative algorithm from the ratio of two potential data with different frequencies [28]–[30]. The reconstruction algorithm of the sensitivity matrix method with the potential difference at two frequencies can also be used [31]–[33]. These two methods principally use the potential difference at two frequencies and a linear reconstruction algorithm.

The relative reconstruction method, apart from using different times and frequencies, can also be done with different objects. In other words, this method can be done by comparing the data of healthy people and sick people. This method has excellent prospective potential as a screening method for certain diseases, such as breast cancer or lung disease.

## 2.2. Design hardware

The development of EIT hardware with neighboring data collection methods is shown in Figure 1. The device consists of several modules, namely an electric current source generator, a data collection module, a potential measuring module, and a microcontroller module. The microcontroller module controls the electrodes that will inject electric current, while the electrodes measure the potential and the measurement data are processed by a computer.

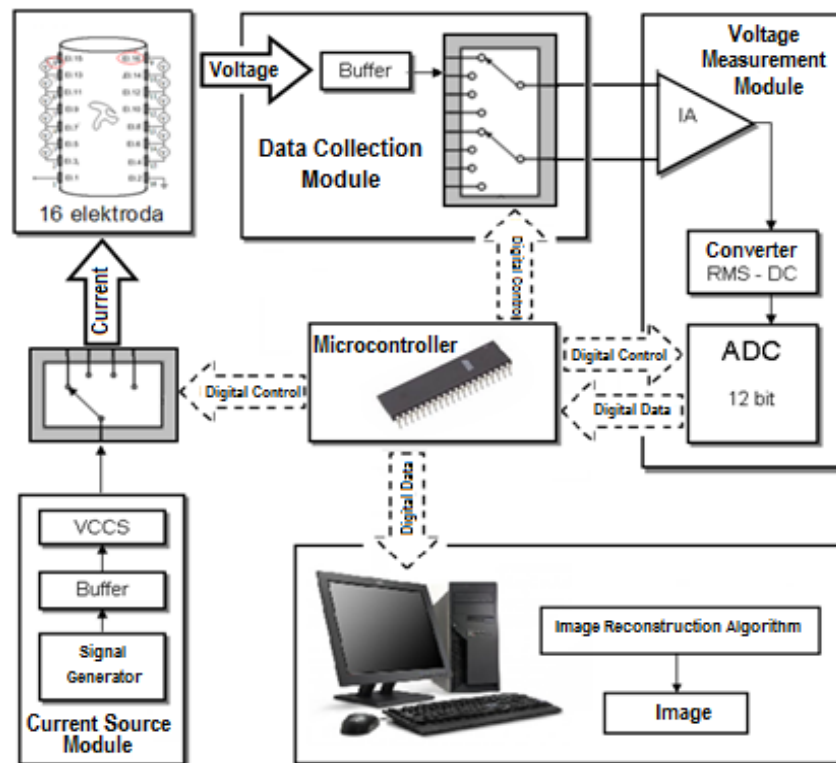


Figure 1. Electrical impedance tomography system development

### 2.3. Phantom and subject

The phantom is made with a tank filled with distilled water and urethane material that is shaped like a lung in the thorax. There are three types of phantoms, namely normal lung, one small hole and one medium hole in the left lung position as shown in Figure 2. Figure 2(a) is a representative of a healthy lung, Figure 2(b) is a representative of small cancer in the lung, and Figure 2(c) is a representative of big cancer in the lung.

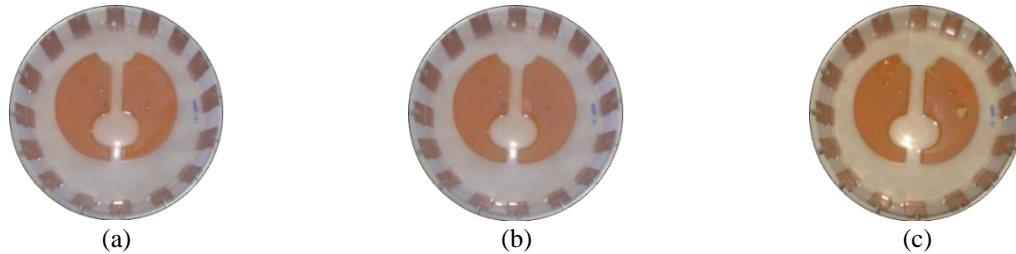


Figure 2. The phantom is made with a tank filled with distilled water and urethane material (a) normal lung, (b) one small hole, and (c) one medium hole in the left lung position

The subjects consisted of one healthy person which is shown in Figure 3 (a) and three patients with lung disease. The patients with lung disease were one with left lung tumor with organized (condensed) left pleural effusion (patient-01) which is shown in Figure 3(b), and one with pulmonary tuberculosis with right pneumothorax (patient-02) which is shown in Figure 3(c) and one with pulmonary tuberculosis with left pleural effusion (patient-03) which is shown in Figure 3(d). The four subjects are shown in Figure 3. Information of the patient conditions were obtained by a radiology doctor based on a chest X-ray of each patient, which is shown in Figure 4. Figure 4(a) is the photothorax of patient-01, Figure 4(b) is the photothorax of patient-02 and Figure 4(c) is the photothorax of patient-03.



Figure 3. The experiment subjects (a) healthy person, (b) patient-01, (c) patient-02, and (d) patient-03

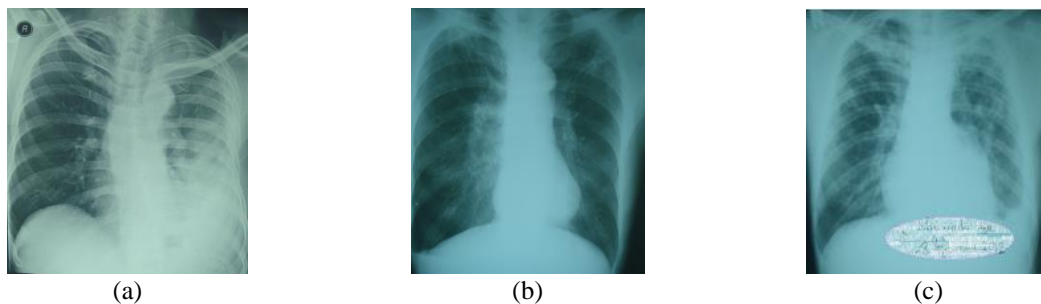


Figure 4. The thorax images of lung patient (a) patient-01, (b) patient-02, and (c) patient-03

### 3. RESULTS AND DISCUSSION

This research started with the design of the EIT device, which is shown in Figure 1. The experiment was conducted by scanning the EIT system on the phantom and thorax. The scanning process was conducted on the three phantoms so that the electrical potential data were obtained which are shown in Figure 5. The reconstruction process was done by the relative method with normal lung phantom potential data as a reference; the results of which are shown in Figure 6. The next experiment was to scan the thorax of one

healthy person and three patients with lung disease. The scanning process was conducted on the four chest cavities under normal breathing, in expiration and inspiration conditions. There were 12 electrical potential data obtained, namely 4 potential data for the four subjects during normal breathing, 4 potential data during inspiration and 4 potential data during expiration. The twelve potential data are shown in Figures 7-10. The reconstruction process was done using the relative method from the twelve potential data. From the reconstruction process, 4 images were generated from the comparison between inspiration and expiration from each person which is shown in Figure 10. Furthermore, there were 9 images from 3 patients in 3 different conditions, namely normal breathing, inspiration and expiration compared to the reference data from the healthy person. The images are shown in Figures 11-13.

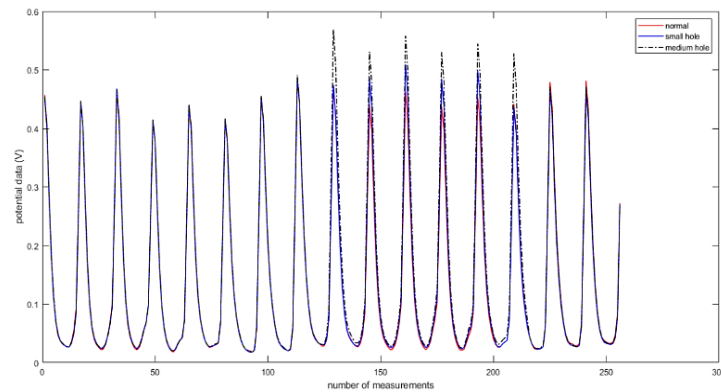


Figure 5. The potential data of normal urethane phantom, small hole and medium hole in the left lung position

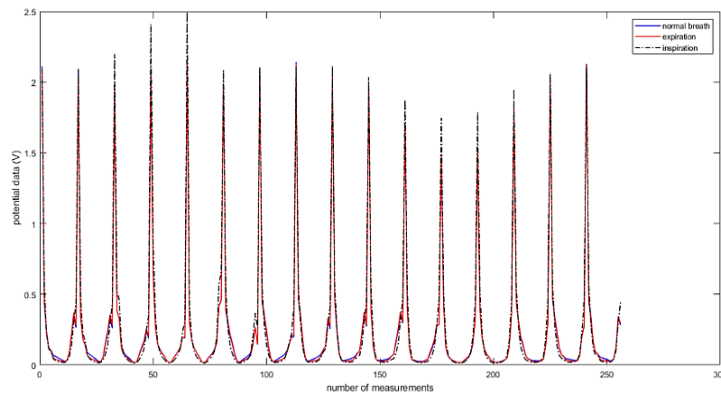


Figure 6. The potential data of healthy person's thorax with normal expiration and inspiration breaths

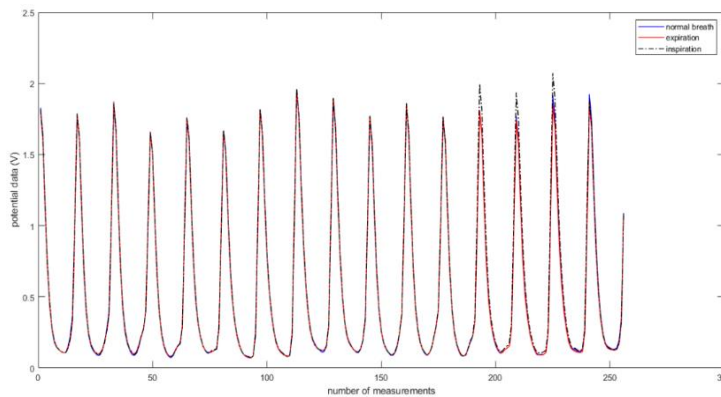


Figure 7. The potential data of a patient-01 with normal expiration and inspiration breaths

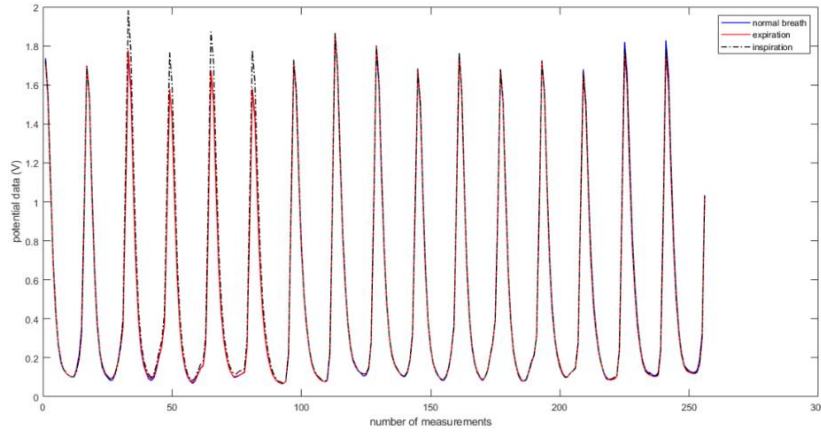


Figure 8. The potential data of a patient-02 with normal expiration and inspiration breaths

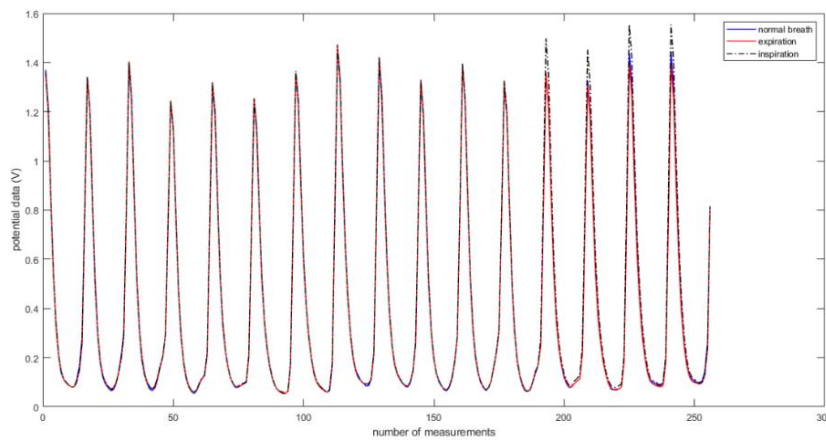


Figure 9. The potential data of patient-03 with normal expiration and inspiration breaths

The study used the relative reconstruction method, namely (6). This equation requires a sensitivity matrix. The matrix is obtained from solving forward problems by the FEM method using 248 elements, with 141 nodes,  $\gamma_0=1$  and  $\delta\gamma=0.05$  [8]. The S matrix is then used in (6) and  $\lambda=10^{-5}$ . By using the sensitivity matrix S and the potential data from Figure 5, it will obtain the reconstruction image on Figure 10.

It shows that the blue color on the left indicates the position of the hole in the urethane on the left for both the small and medium hole urethane objects. Figure 10(a) shows that the size of the blue color is smaller than Figure 10(b), indicating that the hole size of the object (a) is smaller than that of the object (b), which is in accordance with the phantom object. Likewise, with the potential data in Figures 6-9, if they are reconstructed with the same conditions, it will produce the images in Figures 11-14.

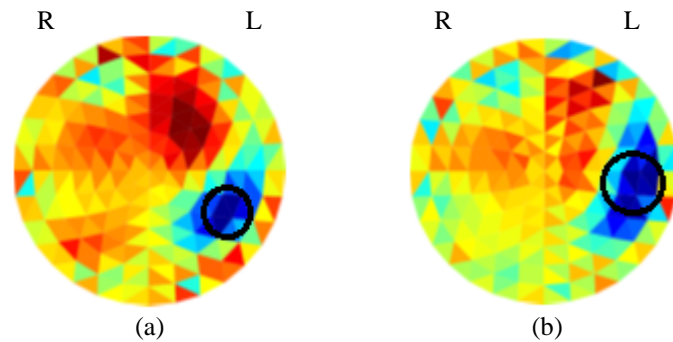


Figure 10. The reconstruction image of (a) the small and (b) medium hole phantom using the relative method with normal phantom as the reference data

The image in Figure 11(a) shows that there is no color difference between the left and right positions of the image. This shows that there is no difference in the lungs of the subject, which is in accordance with the fact that this participant is a healthy person. Meanwhile, in Figures 11(b)-(d), it appears that there is a difference in color between the left and right positions. A blue color indicates that it is a non-uniformity of organs compared to that in a phantom. Figure 11(b) shows the blue color is in the left position of the image, which indicates that the patient 01 has a left lung tumor with an organized (condensed) left pleural effusion. Figure 11(c) shows the blue color is in the right position of the image, which indicates that the patient 02 has pulmonary tuberculosis with right pneumothorax and Figure 11 (d) shows the blue color on the left of the image, which indicates that patient 03 has pulmonary tuberculosis with left pleural effusion.

The Figure 12 shows that there is a difference in the color between the left and right positions. A bluer color indicates that there is a non-uniformity in the organ. Figures 12(a)-(c) the blue color is consistently in the left position, which indicates that patient-01 has a left lung tumor with an organized (condensed) left pleural effusion.

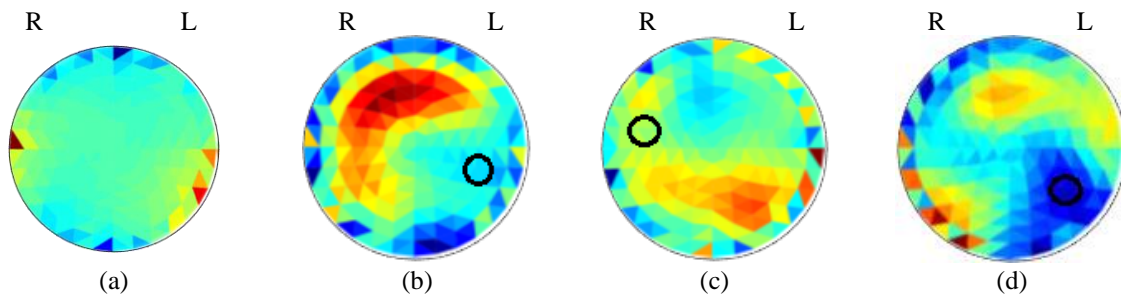


Figure 11. The image reconstruction of potential data during inspiration and expiration as reference for each individual: (a) healthy, (b) patient-01, (c) patient-02, and (d) patient-03

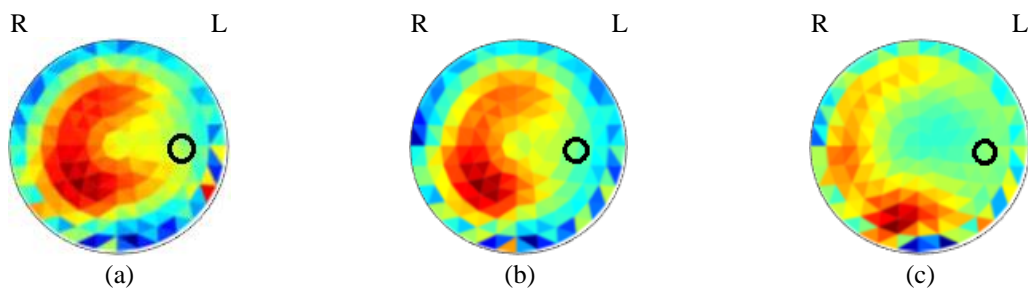


Figure 12. The reconstruction image of patient-01 potential data and healthy as a reference in conditions of (a) normal, (b) expiration, and (c) inspiration breaths

Figure 13 shows that there is a difference in the color between the left and right positions. A bluer color indicates that there is a non-uniformity in the organ. Figures 13(a)-(c) show the blue color is consistently in the right position, which indicates that patient-02 has a condition of pulmonary tuberculosis with right pneumothorax.

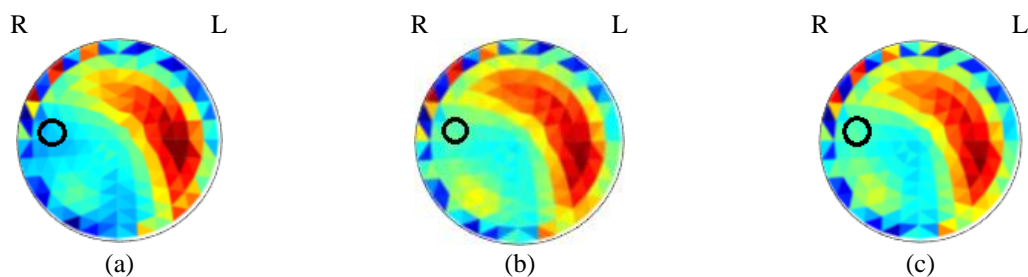


Figure 13. The reconstruction image of patient-02 potential data and healthy as a reference in conditions of (a) normal, (b) expiration, and (c) inspiration breaths

The Figure 14 shows that there is a difference in color between the left and right positions. A blue color indicates that there is a non-uniformity in the organ. Figures 14(a)-(c) show the blue color is consistently in the left position, which is an indication that patient-02 has pulmonary tuberculosis with left pleural effusion.

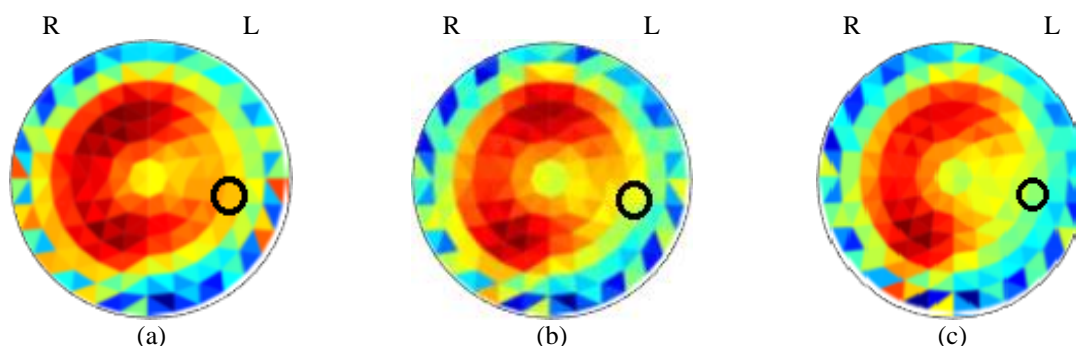


Figure 14. The reconstruction image of patient-03 potential data and healthy as a reference in conditions of (a) normal, (b) expiration, and (c) inspiration breaths

#### 4. CONCLUSION

The relative reconstruction method was used to obtain functional images of the four lungs conditions, which were a healthy person, one with left lung tumor with organized left pleural effusion, one with pulmonary tuberculosis with right pneumothorax and one with pulmonary tuberculosis with left pleural effusion. The relative reconstruction method can be used to obtain functional images of individual lung conditions by using expiratory-respiratory potential data with results that can distinguish between the lungs of a healthy person and a patient with a disease, but the position of the lung disease is seen in less details. Meanwhile, it is important to obtain more accurate functional image information of the lung disease, which can be done by using potential data to compare images between the data of a patient and a healthy person as a reference.

#### ACKNOWLEDGEMENTS

The authors would like to express gratefulness to the Indonesian Ministry of Research and Higher Education for funding this research.

#### REFERENCES

- [1] E. Soya, N. Ekenel, R. Savas, T. Toprak, J. Bewes, and O. Doganay, "Pixel-based analysis of pulmonary changes on CT lung images due to COVID-19 pneumonia," *Cosmoderma*, vol. 12, no. 6, pp. 1–10, 2022, doi: 10.25259/JCIS\_172\_2021.
- [2] X. Li *et al.*, "Electrical-impedance-tomography imaging based on a new three-dimensional thorax model for assessing the extent of lung injury," *AIP Advances*, vol. 9, no. 12, pp. 1–11, 2019, doi: 10.1063/1.5124353.
- [3] K. Ain *et al.*, "Design of electrical impedance tomography for biomedicine," *Journal of Physics: Conference Series*, vol. 1816, no. 1, pp. 1–6, 2021, doi: 10.1088/1742-6596/1816/1/012043.
- [4] D. K. L. Chakraborti and D. W. Selvamurthy, "Clinical application of electrical impedance tomography in the present health scenario of India," *Journal of Physics: Conference Series*, vol. 224, pp. 1–4, 2010, doi: 10.1088/1742-6596/224/1/012069.
- [5] I. Frerichs *et al.*, "Chest electrical impedance tomography examination, data analysis, terminology, clinical use and recommendations: consensus statement of the TRanslational EIT developmeNt stuDy group," *Thorax*, vol. 72, no. 1, pp. 83–93, 2017, doi: 10.1136/thoraxjnl-2016-208357.
- [6] A. G. M. Tharayil, "Review article electrical impedance tomography-watch the lungs breathe!," *Indian Journal of Respiratory Care*, vol. 4, no. 1, pp. 547–553, 2015.
- [7] M. Miedema, I. Frerichs, F. H. C. D. Jongh, M. B. V. Veenendaal, and A. H. V. Kaam, "Pneumothorax in a preterm infant monitored by electrical impedance tomography: a case report," *Neonatology*, vol. 99, no. 1, pp. 10–13, 2011, doi: 10.1159/000292626.
- [8] R. Bhatia, G. M. Schmölzer, P. G. Davis, and D. G. Tingay, "Electrical impedance tomography can rapidly detect small pneumothoraces in surfactant-depleted piglets," *Intensive Care Medicine*, vol. 38, no. 2, pp. 308–315, 2012, doi: 10.1007/s00134-011-2421-z.
- [9] Y. Shi, Z. Yang, F. Xie, S. Ren, and S. Xu, "The research progress of electrical impedance tomography for lung monitoring," *Frontiers in Bioengineering and Biotechnology*, vol. 9, pp. 1–16, 2021, doi: 10.3389/fbioe.2021.726652.
- [10] M. Bodenstern, M. David, and K. Markstaller, "Principles of electrical impedance tomography and its clinical application," *Critical Care Medicine*, vol. 37, no. 2, pp. 713–724, 2009, doi: 10.1097/CCM.0b013e3181958d2f.
- [11] D. Maciejewski, Z. Putowski, M. Czok, and Ł. J. Krzych, "Electrical impedance tomography as a tool for monitoring mechanical

- ventilation. An introduction to the technique,” *Advances in Medical Sciences*, vol. 66, no. 2, pp. 388–395, 2021, doi: 10.1016/j.advms.2021.07.010.
- [12] A. Fagerberg, O. Stenqvist, and A. Åneman, “Monitoring pulmonary perfusion by electrical impedance tomography: an evaluation in a pig model,” *Acta Anaesthesiologica Scandinavica*, vol. 53, no. 2, pp. 152–158, 2009, doi: 10.1111/j.1399-6576.2008.01847.x.
- [13] J. Riera, P. J. Riu, P. Casan, and J. R. Masclans, “Electrical impedance tomography in acute lung injury,” *Medicina Intensiva (English Edition)*, vol. 35, no. 8, pp. 509–517, 2011, doi: 10.1016/j.medicine.2011.11.004.
- [14] B. Harrach and J. K. Seo, “Exact shape-reconstruction by one-step linearization in electrical impedance tomography,” *SIAM Journal on Mathematical Analysis*, vol. 42, no. 4, pp. 1505–1518, 2010, doi: 10.1137/090773970.
- [15] B. Brazey, Y. Haddab, and N. Zemiti, “Robust imaging using electrical impedance tomography: review of current tools,” *Proceedings of the Royal Society A: Mathematical, Physical and Engineering Sciences*, vol. 478, no. 2258, pp. 1–22, 2022, doi: 10.1098/rspa.2021.0713.
- [16] V. Tomicic and R. Cornejo, “Lung monitoring with electrical impedance tomography: technical considerations and clinical applications,” *Journal of Thoracic Disease*, vol. 11, no. 7, pp. 3122–3135, 2019, doi: 10.21037/jtd.2019.06.27.
- [17] I. Sapuan, K. Ain, and A. Suryanto, “Dual frequency electrical impedance tomography to obtain functional image,” *Journal of Physics: Conference Series*, vol. 853, pp. 1–11, 2017, doi: 10.1088/1742-6596/853/1/012002.
- [18] X.-Y. Ke *et al.*, “Advances in electrical impedance tomography-based brain imaging,” *Military Medical Research*, vol. 9, no. 1, pp. 1–22, 2022, doi: 10.1186/s40779-022-00370-7.
- [19] K. Ain, D. Kurniadi, Suprijanto, and O. Santoso, “Lungs anomaly detection by filtered back projection reconstruction method in electrical impedance tomography,” in *2013 3rd International Conference on Instrumentation Control and Automation (ICA)*, 2013, pp. 133–137, doi: 10.1109/ICA.2013.6734059.
- [20] A. Borsic, “Regularisation methods for imaging from electrical measurements,” Oxford Brookes University, 2002.
- [21] J. A. E. Noor, “Electrical impedance tomography at low frequencies,” Universitas New South Wales Sydney, 2007.
- [22] X. Y. Chen, H. X. Wang, and J. C. Newell, “Lung ventilation reconstruction by electrical impedance tomography based on physical information,” in *2011 Third International Conference on Measuring Technology and Mechatronics Automation*, 2011, pp. 489–492, doi: 10.1109/ICMTMA.2011.409.
- [23] R. Kulkarni, G. Boverman, D. Isaacson, G. J. Saulnier, T.-J. Kao, and J. C. Newell, “An analytical layered forward model for breasts in electrical impedance tomography,” *Physiological Measurement*, vol. 29, no. 6, pp. 27–40, 2008, doi: 10.1088/0967-3334/29/6/S03.
- [24] N. K. Soni, A. Hartov, C. Kogel, S. P. Poplack, and K. D. Paulsen, “Multi-frequency electrical impedance tomography of the breast: new clinical results,” *Physiological Measurement*, vol. 25, no. 1, pp. 301–314, 2004, doi: 10.1088/0967-3334/25/1/034.
- [25] O. V. Trokhanova, M. B. Okhapkin, and A. V. Korjenevsky, “Dual-frequency electrical impedance mammography for the diagnosis of non-malignant breast disease,” *Physiological Measurement*, vol. 29, no. 6, pp. 331–344, 2008, doi: 10.1088/0967-3334/29/6/S28.
- [26] C. Gabriel, S. Gabriel, and E. Corthout, “The dielectric properties of biological tissues: I. literature survey,” *Physics in Medicine and Biology*, vol. 41, no. 11, pp. 2231–2249, 1996, doi: 10.1088/0031-9155/41/11/001.
- [27] T. I. Oh *et al.*, “Validation of a multi-frequency electrical impedance tomography (mfEIT) system KHU Mark1: impedance spectroscopy and time-difference imaging,” *Physiological Measurement*, vol. 29, no. 3, pp. 295–307, 2008, doi: 10.1088/0967-3334/29/3/002.
- [28] H. Griffiths and A. Ahmed, “A dual-frequency applied potential tomography technique: computer simulations,” *Clinical Physics and Physiological Measurement*, vol. 8, no. 4A, pp. 103–107, 1987, doi: 10.1088/0143-0815/8/4A/014.
- [29] H. Griffiths and Z. Zhang, “A dual-frequency electrical impedance tomography system,” *Physics in Medicine and Biology*, vol. 34, no. 10, pp. 1465–1476, 1989, doi: 10.1088/0031-9155/34/10/009.
- [30] J. Schlappa, E. Annese, and H. Griffiths, “Systematic errors in multi-frequency EIT,” *Physiological Measurement*, vol. 21, no. 1, pp. 111–118, 2000, doi: 10.1088/0967-3334/21/1/314.
- [31] A. Romsauerova, A. McEwan, L. Horesh, R. Yerworth, R. H. Bayford, and D. S. Holder, “Multi-frequency electrical impedance tomography (EIT) of the adult human head: initial findings in brain tumours, arteriovenous malformations and chronic stroke, development of an analysis method and calibration,” *Physiological Measurement*, vol. 27, no. 5, pp. 147–161, 2006, doi: 10.1088/0967-3334/27/5/S13.
- [32] R. J. Yerworth, R. H. Bayford, B. Brown, P. Milnes, M. Conway, and D. S. Holder, “Electrical impedance tomography spectroscopy (EITS) for human head imaging,” *Physiological Measurement*, vol. 24, no. 2, pp. 477–489, 2003, doi: 10.1088/0967-3334/24/2/358.
- [33] J. K. Seo, J. Lee, S. W. Kim, H. Zribi, and E. J. Woo, “Frequency-difference electrical impedance tomography (fdEIT): algorithm development and feasibility study,” *Physiological Measurement*, vol. 29, no. 8, pp. 929–944, 2008, doi: 10.1088/0967-3334/29/8/006.

## BIOGRAPHIES OF AUTHORS



**Lina Choridah**    is a lecturer at the Department of Radiology, Faculty of Medicine, Public Health and Nursing, Universitas Gadjah Mada and also Vice Dean for Research and Development. She received her doctorate degree from UGM in 2013 and is a Radiology Consultant of Breast and Gynecology Imaging. In addition to woman imaging, she is also an experienced expert in the field of artificial intelligence and medical device development. She can be contacted at email: linachoridah@ugm.ac.id or linailmiah@gmail.com.



**Riries Rulaningtyas**    is a senior lecturer in Biomedical Engineering, Department of Physics, Faculty of Science and Technology, Universitas Airlangga, Indonesia. She got her bachelor and master degrees from the Institut Teknologi Sepuluh Nopember, Surabaya. She received her Ph.D degree in Biomedical Engineering, Institut Teknologi Bandung. Her research interests are medical image processing, medical signal processing, and artificial intelligence. She can be contacted at email: riries-r@fst.unair.ac.id.



**Lailatul Muqmiroh**    is a lecturer at Applied Bachelor of Radiologic Imaging Technology, Faculty of Vocational Studies, Airlangga University, Indonesia. She received her Bachelor degree at Medical Faculty of Brawijaya University, Indonesia in 2000, and her master's degree at the Medical Faculty of Airlangga University majoring in Radiology in 2010. Recently, she is a doctoral student of Medical Faculty at Airlangga University. Her research fields are diagnostic imaging, image processing, and interventional radiology. She can be contacted at email: lailatul.muqmiroh@vokasi.unair.ac.id.



**Suprayitno**    received his bachelor's degree in 1997 from the Department of Physics, Faculty of Science and Technology, Airlangga University, and master degrees in 2011 from Information Technology Management, Sepuluh Nopember Institute of Technology. All of them are in Surabaya, Indonesia. His current research interests include microcontrollers, image processing and the Internet of things. He can be contacted at email: suprayitno-2017@fst.unair.ac.id or prayit.suprayitno.sp@gmail.com.



**Khusnul Ain**    is a senior lecturer in Bachelor of Biomedical Engineering, Department of Physics, Faculty of Science and Technology, Airlangga University, Indonesia. He got his bachelor, master, and doctoral degree from Universitas Gadjah Mada majoring Nuclear Engineering, Physics, and Bandung Institute of Technology majoring Physics Engineering. All of them are in Indonesia. His research field are tomography and spectroscopy of electrical bioimpedance. He can be contacted at email: k\_ain@fst.unair.ac.id.